Macromolecules

ARTICLE

pubs.acs.org/Macromolecules

Structural Regularization in the Crystallization Process from the Glass or Melt of Poly(L-lactic Acid) Viewed from the Temperature-Dependent and Time-Resolved Measurements of FTIR and Wide-Angle/Small-Angle X-ray Scatterings

Kaewkan Wasanasuk and Kohji Tashiro*

Department of Future Industry-oriented Basic Science and Materials, Graduate School of Engineering, Toyota Technological Institute, Tempaku, Nagoya 468-8511, Japan

ABSTRACT: Structural evolution has been traced in the crystallization process of poly(L-lactic acid) (PLLA) from the melt or from the glass by measuring the FTIR spectra, wide-angle X-ray diffraction (WAXD), and small-angle X-ray scattering (SAXS) patterns as functions of temperature or time. Using the infrared bands characteristic of the melt, mesomorphic phase (mesophase) and crystalline phase as well as the WAXD 200/110 and 0010 reflections and the SAXS long-period peak, the regularization processes were analyzed systematically from the different points of view. In the case of cold-crystallization from the glass, the mesophase was found to regularize into the disordered α (α' or δ) form in the temperature region from just above the glass transition point (Tg, 70 °C) to 120 °C, whereas it changed to the regular α form in the higher temperature region. On the other hand, in the melt-crystallization process, the crystallization to the α or δ form occurred *not directly from the melt* but *via the mesophase from the melt*. In this way the isothermal crystallizations from the glass and from the melt were found to occur always with the first appearance of the mesophase from the amorphous phase followed by the transition to the crystalline α or δ phase. The 2-dimenisonal X-ray diffraction diagram was analyzed to investigate the structure of the oriented mesophase, in which the conformationally disordered (10/3) helical chains are gathered together with low correlation to form a small domain of about 30 Å (c axis) × 20 Å (lateral direction) size. In the cold crystallization process, these small domains of the mesophase grew larger to form the domains of the δ form of 75 × 100 Å size, attendant with the imperfect conformational regularization as well as the disorder in relative height between the neighboring domains. By increasing the temperature furthermore, the δ form transforms to the α form consisting of the more tightly packed chains of regular conformation in the domain of about 170 × 300 Å size. In this way, the thermally induced regularization of PLLA was found to occur in a complicated manner: from the glass to the mesophase, to the δ form and to the α form in the cold crystallization phenomenon of the melt-quenched sample, while it occurs from the melt to the mesophase and to the α or δ form in the cooling process from the melt.

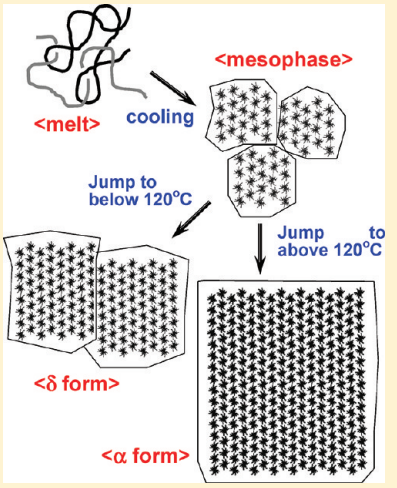

INTRODUCTION

Poly(L-lactic acid) (PLLA) is now attracting many attentions because of its possibility for the practical usages as one of the general multipurposes polymer materials. However, there are many problems to be clarified including the relatively poor mechanical property, the relatively low melting point and so on.[1,2] Among these problems, the slow crystallization rate in the melt processing is one of the most serious problems in the industrial point of view.[1,2] As one important factor, the existence of D-lactic acid units in PLLA chains as a contaminant is said to reduce the melt-crystallization rate by one order or higher.[3] It might be easy to speculate that the inclusion of different type of comonomer units disturbs the formation of regular helical sequences along the chain axis, resulting in the poor crystallization. However, there have been quite limited number of reports which describe concretely and in detail the structural evolution process itself in the crystallization of PLLA. Most of these papers investigated the crystallization behaviors from the melt or glass by measuring the thermal behavior or by observing the optical microscopic images of the spherulites.[4−31]

At first let us review these previous studies about the cold crystallization from the glassy sample, which is prepared by quenching the melt into ice−water temperature.[13−15,17,21,24−26,28] The thus-obtained glassy sample is not necessarily in the perfectly amorphous state but some parts are more or less ordered in the chain aggregation mode.[32−37] This sample is called the mesomorphic phase or mesophase.[36] Stoclet et al. measured the X-ray diffraction pattern of the stretched PLLA glass containing 4 mol % D component and proposed the partially ordered liquid-crystal-like structure for the mesophase of PLLA.[32,33] But the detailed structure

Received: July 31, 2011
Revised: October 17, 2011
Published: November 21, 2011

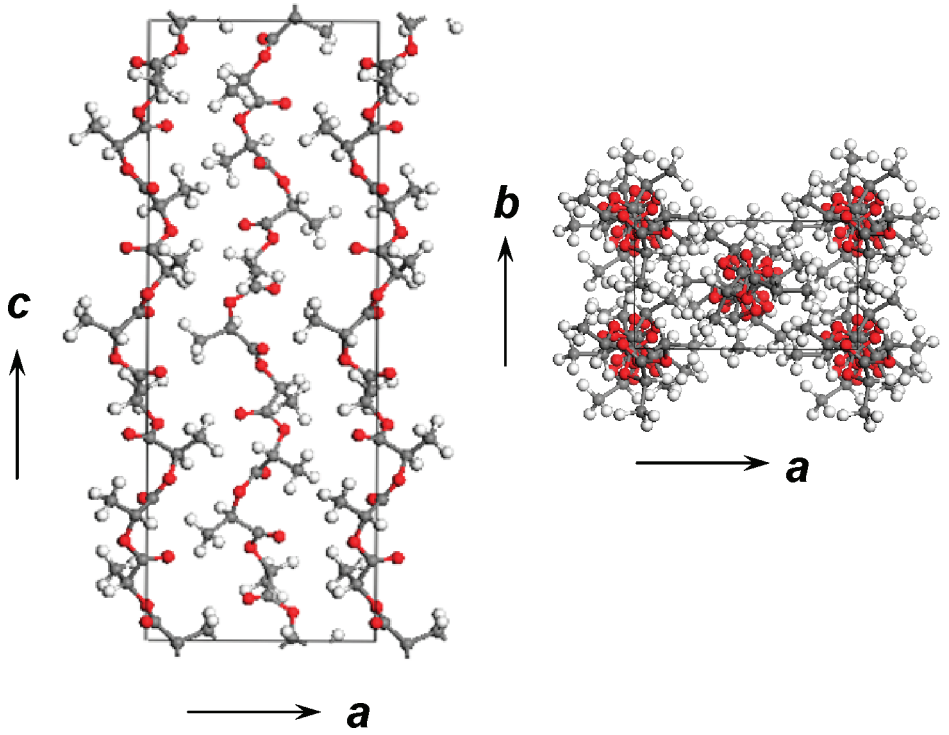

Figure 1. Crystal structure of PLLA α form.[41].

of the mesophase has not yet been clarified. Mano et al.,[8,9] Stoclet et al.[32,33] and Iannace and Nicolas[17] speculated the existence of the rigid amorphous state in addition to the mobile amorphous state, in which the former seems to correspond to the mesophase although they did not mention it explicitly. The content of the rigid amorphous state was evaluated by analyzing the heat capacity change in the glass transition temperature region and the X-ray halo peak. The rigid amorphous state in the quenched sample was found to decrease by annealing above 110 °C.[17] Correspondingly, the X-ray crystalline peaks started to appear. FTIR and Raman spectral studies revealed also the regularization of the mesophase.[34,35,37] The crystallization rate from the mesophase was measured, which was classified into three regimes: the regime I below 113 °C, the regime II between 113 and 135 °C, and the regime III above 135 °C.[8,16−20,23] The samples crystallized in the regimes I and II showed the two DSC endothermic peaks, while the sample in regime III showed a single endothermic peak. These multiple peaks were assigned tentatively to the melt-recrystallization of the α phase. However, when the mesophase sample was annealed at around 115 °C, the sample was found to show the X-ray diffraction pattern and infrared spectra different from those of the original mesophase and the α form.[4−7,38−45] This crystalline phase was named the α' form (or the δ form in the present paper), the structure of which should be more disordered in the conformation and packing mode of chains when compared with the crystal structure of the α form (see Figure 1).[41] The temperature-dependent X-ray diffraction measurement revealed that this α' phase shows the disorder-to-order phase transition to the α form followed by the melting of the α form.[14,42−45] These two transition processes give the double endothermic peaks in the DSC thermograms. The crystal structure of the α' (δ) form has not yet been clarified in detail.[42]

The similar discussion was made also for the melt-isothermal crystallization phenomenon.[16−31] The crystallization growth rate was plotted against the isothermal crystallization temperature *Tc*.[5,8−10,16−20,23,30,40] Miyata and Masuko revealed the existence of the maximal peak at around 120 °C.[30] Di Lorenzo et al. measured the crystallization growth rate in more detail and found the double maximal peaks at *Tc* = 115 and 130 °C.[18] Inoue et al.[10,40] and Kawai et al.[5] reported the similar results. As already mentioned above, the sample crystallized at around 115 °C was identified as the α' phase.[4−7,38−45] The higher crystallization temperature gave the regular α form. The structure change in the crystallization from the melt also has not yet been clarified enough well. In the case of polyethylene, for example, the crystallization from the melt does not occur directly into the orthorhombic crystalline phase but *via* the intermediate phase consisting of the conformationally disordered trans chain segments or the hexagonal phase, as revealed by Tashiro et al. through the time-resolved measurement of WAXD, SAXS and FTIR spectra in the isothermal crystallization process.[46] This intermediate phase may be called also the mesophase. Strobl deduced the image of crystallization of lamellae where the amorphous chain segments are adsorbed on the end surface of growing lamella and form the intermediate phase which is regularized into the orthorhombic phase as the time passes.[47] They applied this model to the melt-crystallization process of PLLA *via* the mesophase.[7] But, almost no experimental evidence was presented to provide the participation of the mesophaseon the way of crystallization of PLLA from the melt.

In this way the structural changes from the melt or from the glass of PLLA have not yet been clarified satisfactorily. In the present paper we will describe the crystallization behavior of PLLA from the microscopic viewpoint by performing the temperature-dependent and/or time-dependent measurements

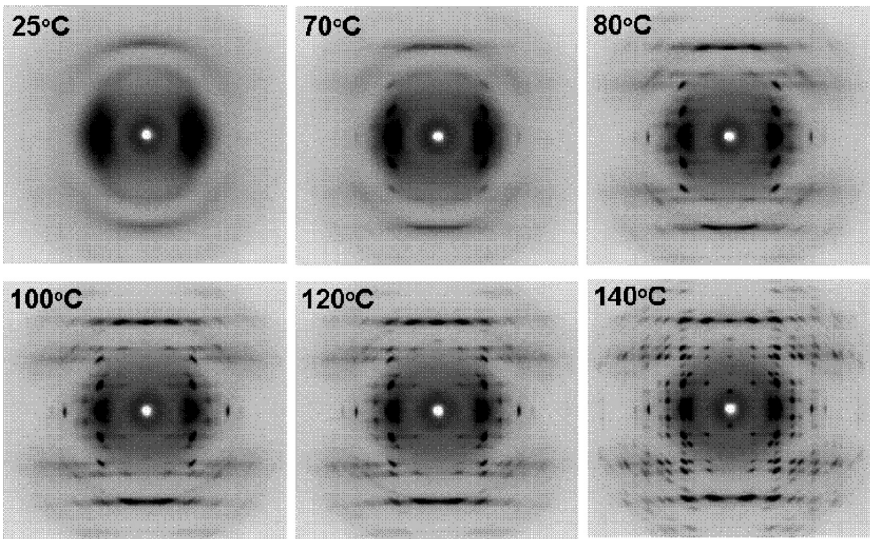

Figure 2. Temperature dependence of 2D X-ray diffraction diagrams of the oriented PLLA mesophase measured in the heating process.

of the WAXD, SAXS and FTIR data. As known already, the crystallization from the melt into the α or δ form is dependent on the crystallization temperature, but our important conclusion is that the crystallization occurs always *via the mesomorphic phase (mesophase) consisting of the small domains with disordered packing of (10/3) helical chains*, as will be described in a later section. Another new information obtained from the IR data analysis is that the melt-quenched sample is not necessarily in the perfectly amorphous state but it forms the mesophase, which regularizes at higher rate to the α form *via* the disordered δ form. These new insights will make a large contribution to the study of the control of crystallization behavior of PLLA.

EXPERIMENTAL SECTION

Samples. PLLA samples were supplied kindly by Professor Tsuji, Toyohashi University of Technology. The averaged molecular weight was 600,000 g/mol with the polydispersity 1.9. The thin films of ca. 40 μm thickness were prepared by casting from the chloroform solution at room temperature. These films were melted at 220 °C and cooled rapidly to ice water bath to obtain the glassy sample. The oriented mesophase sample was prepared by stretching the melt-quenched sample 4 times the original length at 60 °C.

X-ray Diffraction Measurements. The temperature dependence of the 2-dimensional X-ray diffraction diagrams was measured for the uniaxially oriented samples by irradiating a graphite-monochromatized Mo−Kα X-ray beam generated from a Rigaku R-axis VII X-ray diffractometer equipped with flat imaging plates as detector. The temperature dependence of the meridional *00 L* reflections was measured in a transmission mode using a Rigaku TTR-III X-ray diffractometer where the Cu−Kα line was used as an incident X-ray beam. The crystallite sizes were estimated based on the Scherrer's equation using the half-widths of the corresponding X-ray reflections after the correction of the instrumental broadening.[48]

FTIR Measurements. The time-dependence of FTIR spectral changes was measured during the isothermal crystallization from the melt or from the glass using a Varian FTS7000 rapid-scanning infrared spectrometer. The temperature jump from the melt to a crystallization temperature (Tc) or from the glassy state to Tc was performed using a homemade optical cell specialized for the temperature jump experiment. The temperature jump rate was ca. 90 °C/min for the heating experiment and ca. 600 °C/min for the cooling experiment. The FTIR spectra were measured every 2 - 7 s in these processes.

Simultaneous FTIR/WAXD/SAXS Measurements. The transmission-type Fourier-transform infrared spectra (FTIR), wide-angle X-ray diffraction (WAXD) and small-angle X-ray scattering (SAXS) were measured simultaneously using a synchrotron X-ray beam at SPring-8 beamline BL40XU during the isothermal crystallization of the unoriented mesophase sample at Tc = 130 °C. The wavelength of an incident X-ray beam of about 100 × 200 μm size was 0.827 Å. The IR, WAXD and SAXS data were collected at every 10 s in the temperature jump from 25 °C to Tc. The details of the experimental system will be reported elsewhere.[49]

Computer Simulation of X-ray Diffraction Patterns. The 2-dimensional X-ray diffraction pattern and the layer line profiles were calculated using a commercial software Cerius^2 (version 4.6, Accelrys Inc.) on the basis of the structure derived by the X-ray diffraction analysis.

RESULTS AND DISCUSSION

Cold Crystallization from the Glass. *Temperature Dependence.* Figure 2 shows the temperature dependence of the 2D X-ray diffraction diagram of uniaxially oriented PLLA sample starting from the oriented mesophase. The reflections of the mesophase are totally broad and diffuse, but these reflection positions are almost the same as those predicted for the δ and α forms obtained in higher temperature region. The strong equatorial spot of the lattice spacing 5.77 Å is detected, corresponding to the 200/110 reflection of the δ and α forms.[5−7,41,42] The crystallite size estimated by the Scherrer's equation[48] is about 20 Å. The observed layer line reflections are quite diffuse but similar to those of the oriented α and δ forms, indicating that the molecular chains in the mesophase may take the (10/3) helical conformation.[41,42] The lattice size along the chain axis is estimated to be ca. 30 Å from the half-width of the 0010 reflection (see Figure 4). From these observations the mesophase is speculated to exist as the small domain of 30 Å ($\parallel$ c axis) × 20 Å (lateral direction) size, in which the more or less disordered (10/3) helical chains are packed with the low degree of regularity. However, Figure 3 tells us that the X-ray diffraction pattern of the mesophase is rather similar to that of an isolated PLLA chain. This indicates that the molecular chains in the mesophase are not

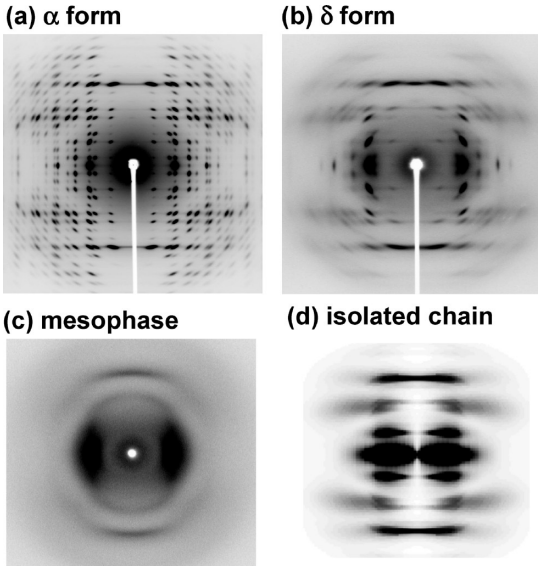

Figure 3. Observed X-ray diffraction diagrams of PLLA (a) α form, (b) δ form, (c) mesophase, and (d) the X-ray diffraction pattern calculated for an isolated single chain of (10/3) helical conformation.

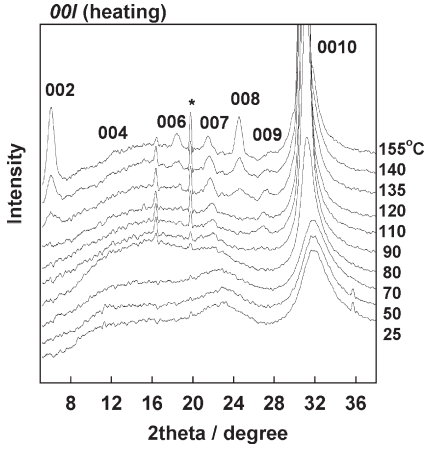

Figure 4. Temperature dependence of the 00*L* reflection profile measured in the heating process from the oriented PLLA mesophase. The peak with asterisk is due to the noise.

regularly packed but they have quite low correlation from each other.

By heating the mesophase sample to the temperature just beyond the glass transition point (*Tg*, 70 °C), the X-ray diffraction pattern became clearer, and several reflection spots were detected at the positions corresponding to those of the δ form.[6,42] The packing structure of the δ form was recently clarified on the basis of the X-ray structure analysis.[42] As the temperature increased furthermore, the diffuse layer lines became more spot-like patterns and the whole X-ray diffraction pattern approached finally to that of the regular α form (see Figure 3). Figure 4 shows the temperature dependence of the 00*L* reflection profile measured for the oriented mesophase in the transmission mode. The pattern was found to change at the two stages. At the room temperature the mesophase gives the broad peaks but the 0010 reflection can be detected clearly though a little broader. The repeating period along the chain axis,

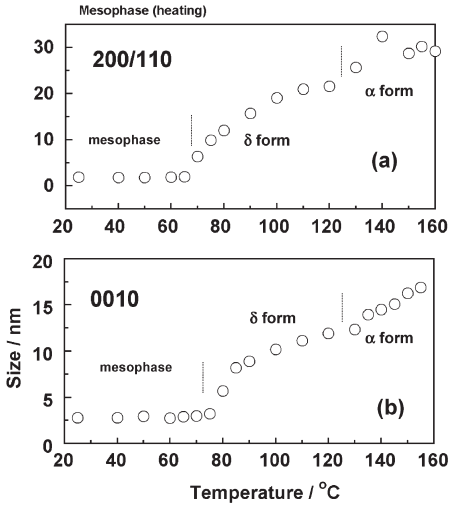

Figure 5. Temperature dependence of the crystallite sizes estimated for the oriented PLLA crystalline forms along the *a*- and *c*-axes in the heating process starting from the mesophase.

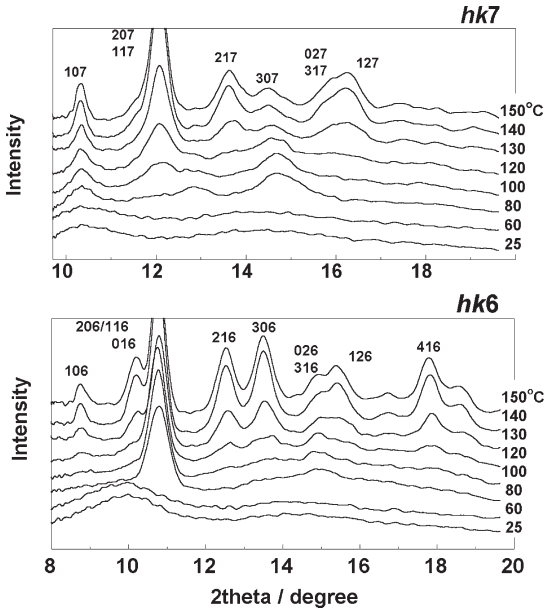

Figure 6. Temperature dependence of the X-ray diffraction profiles along the 6th and 7th layer lines detected for the oriented PLLA sample in the heating process from the mesophase (refer to Figure 2).

ca. 28.0 Å, is shorter than those of the δ (28.8 Å)[42] and α forms (28.9 Å).[41] As the temperature increases above T_g (70 °C), some peaks were detected to appear, the whole profile of which is that of the δ form.[42] In the higher temperature region than 120 °C, the sharper peaks of 002, 008, and so on were detected clearly, corresponding to those of the α form.[41] The crystallite sizes along the *a* and *c* axial directions, estimated from the half-widths of the 200/110 and 0010 reflections, are plotted against temperature as shown in Figure 5, parts a and b, respectively. The crystallite size increased steeply above *Tg* and finally reached the values of 170 Å ($\parallel$ *c* axis) × 300 Å ($\parallel$ *a* axis) in the α form. The temperature dependences of the *hk6* and *hk7* layer line reflections are shown in Figure 6. The changes occurred at the 2 steps as pointed out above. The first change was detected at

dx.doi.org/10.1021/ma2017666 |*Macromolecules* 2011, 44, 9650–9660

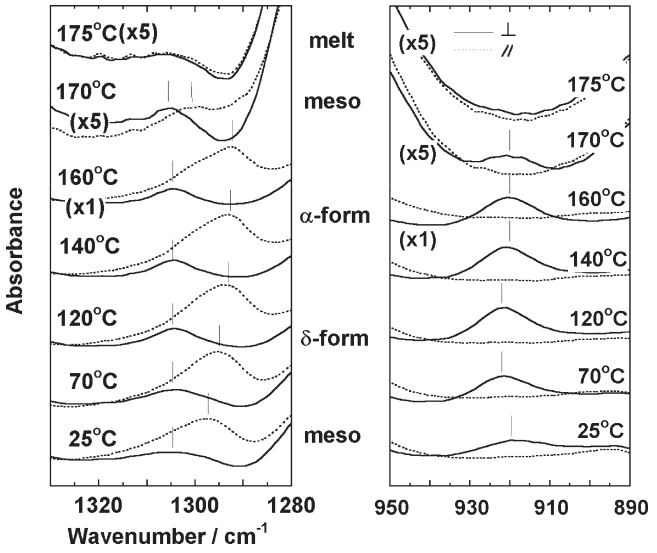

Figure 7. Temperature dependence of polarized infrared spectra measured for oriented PLLA mesophase in the heating process: (—) the electric vector of an incident IR beam perpendicular to the orientation direction; (--) the electric vector of an incident IR beam parallel to the orientation direction.

around T_g from the mesophase with broad profiles to the δ form with broad but some spot-like reflections. The second change started to occur at around 120 °C, where the δ form having smaller number of reflections changed to the α form with many sharper reflections.

Figure 7 shows the polarized infrared spectra measured for the oriented mesophase sample in the heating process. The perpendicularly polarized band at 919 cm^{-1}, for example, was broad but highly polarized in the mesophase at 25 °C, which increased the intensity and shifted to the position at 922 cm^{-1} in the δ form above 70 °C. The peak position changed again to the 920 cm^{-1} in the temperature region higher than 120 °C or the α form. This band disappeared perfectly in the molten state. The parallel-polarized band at 1297 cm^{-1} and the perpendicularly polarized band 1304 cm^{-1} are also assigned to the mesophase at room temperature, which shifted to 1294 and 1303 cm^{-1} and increased in intensity above T_g or in the δ form. The 1294 cm^{-1} band shifted to 1293 cm^{-1} in the α form region, and disappeared in the melt. Before we finish the description of the IR spectral change, it must be noticed here that the polarized IR spectra measured at 170 °C or immediately below the melting point were quite different from those of the α form and they were rather similar to those of the starting mesophase. The spectra kept the polarization character, indicating an appearance of the oriented mesophase before the melt.

In the above discussion only the oriented glassy sample was used. The unoriented glass was prepared easily by quenching the melt into an ice−water bath. This sample was heated up to the melting point at 2 °C/min rate, during which the X-ray diffraction profiles were measured. This glassy sample changed to the δ form in the temperature region from above T_g to 120 °C, and then the δ form transformed to the α form in the higher temperature region of ca. 160 °C.[44]

Time Dependence. Figure 8 shows the time-dependence of the infrared spectra measured in the isothermal crystallization process starting from the glassy sample at room temperature.

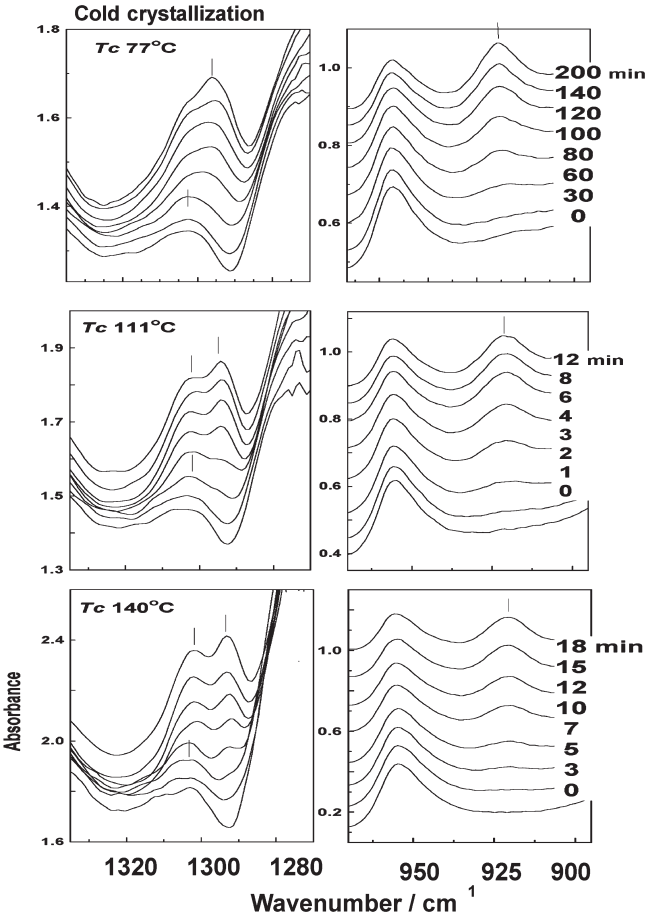

Figure 8. Time dependence of infrared spectra of PLLA mesophase measured in the isothermal crystallization process at constant temperature T_c.

The cases of the crystallization temperatures (T_c) 77, 111, and 140 °C are given here. As already pointed out the peak positions of the bands are dependent on the aggregation states of the chains. Strictly speaking the band positions of the oriented (Figure 7) and unoriented samples (Figure 8) are different apparently because of the overlapping effect of the neighboring bands, but we can utilize these bands for the discussion of regularization processes of the glassy sample. As the crystallization was proceeded at 77 °C just above the T_g, the 920 cm^{-1} band intrinsic to the mesophase increased in intensity at around 60 min after the temperature jump and the 922 cm^{-1} band of the δ form started to appear and increased the intensity with time. At the same time the δ-form band at 1297 cm^{-1} started to appear as a shoulder and increased in intensity with the passage of time. These behaviors became more remarkable and the crystalline-sensitive bands appeared at 922 cm^{-1} more rapidly at 111 °C. The δ-form bands at 1294 and 1302 cm^{-1} were also detected at the same time. The sharp bands at 1293 and 1302 cm^{-1} intrinsic to the α form increased in intensity a little slower at 140 °C compared with the case of 111 °C. The normalized intensity evaluated for the crystallization-sensitive band at 920 cm^{-1} is plotted against time in Figure 9a. The crystallization rate constant k in the Avrami equation $X = X_o(1 - \exp[(-kt)^n])$ was estimated and plotted against the crystallization temperature in Figure 10. The constant k is found to show a peak at around

dx.doi.org/10.1021/ma2017666 |*Macromolecules* 2011, 44, 9650–9660

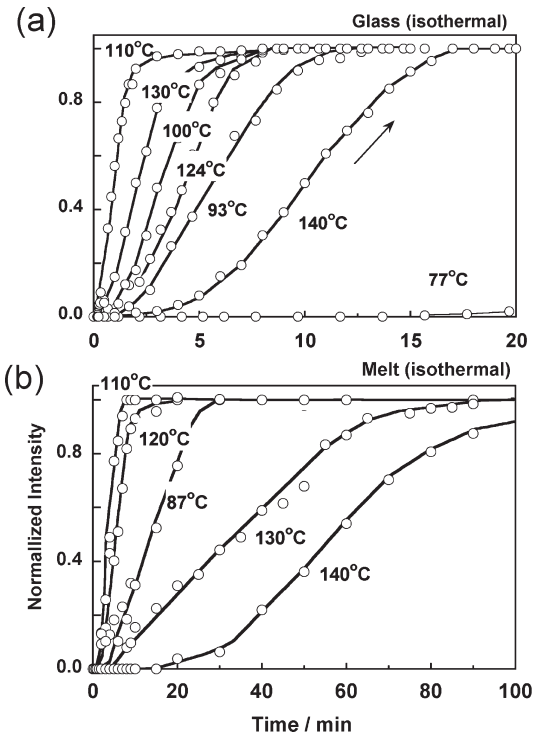

Figure 9. Time dependence of normalized intensity of the crystallization-sensitive 921 cm^{-1} band measured in the isothermal crystallization processes at the various T_c.

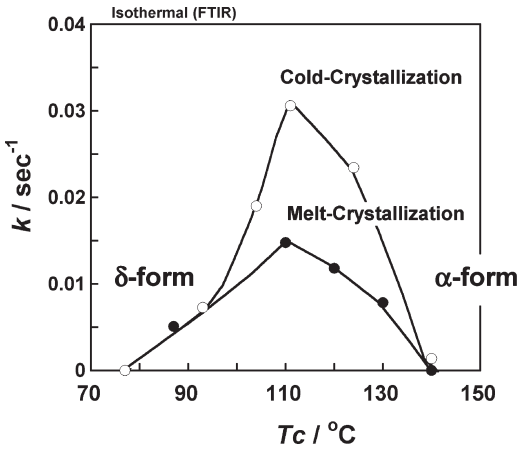

Figure 10. Crystallization temperature dependence of the crystallization rate constant k estimated for the PLLA samples in the melt- and cold-crystallization processes.

110 °C, corresponding to the faster crystallization rate of the δ form in the region 100−120 °C. The cold crystallization in the higher temperature region induced the formation of the α form and the crystallization rate became slower.

The regularization process from the unoriented mesophase was traced also by performing the simultaneous measurement of FTIR spectra and WAXD/SAXS patterns using a newly developed system, the details of which will be reported elsewhere.[49] The measurement was performed at BL40XU in SPring-8. Figures 11 and 12 show, respectively, the time dependence of SAXS/WAXD and FTIR spectra measured simultaneously in the

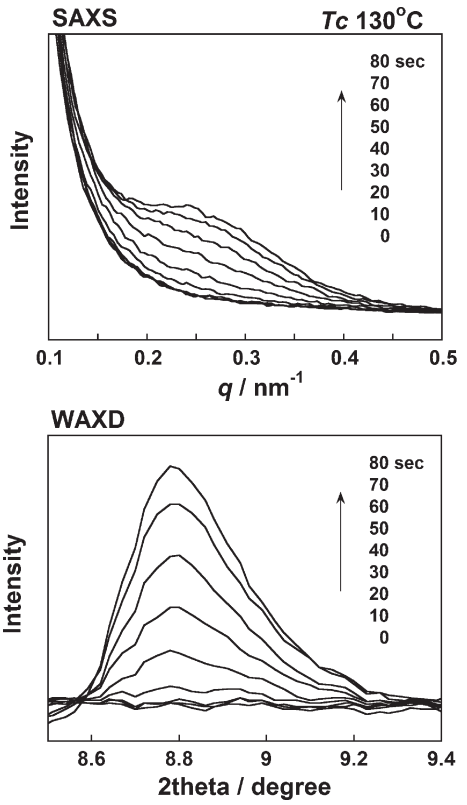

Figure 11. Time dependence of SAXS and WAXD profiles of unoriented PLLA mesophase sample measured in the isothermal crystallization process at 130 °C.

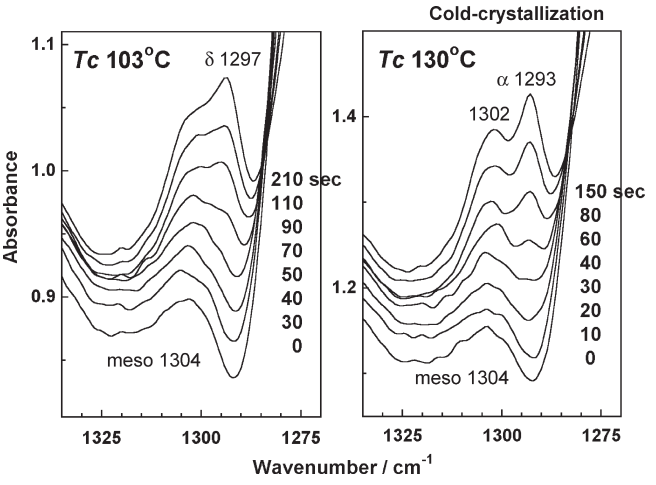

Figure 12. Time dependence of infrared spectra of unoriented PLLA mesophase sample measured in the isothermal crystallization process at 103 and 130 °C.

isothermal crystallization at 103 and 130 °C, respectively. The SAXS data obtained in the early stage of the crystallization were analyzed on the basis of the scattering equation[50,51] in the low q range to estimate the radius of gyration R_g of the small nodules speculated to exit in the mesophase, where q is a scattering vector defined as $q = (4\pi/\lambda)\sin(\theta)$ (λ, X-ray wavelength, 0.83 Å; 2θ, the scattering angle). The long period of the stacked lamellar structure started to be detected after some time passage.

dx.doi.org/10.1021/ma2017666 |*Macromolecules* 2011, 44, 9650–9660

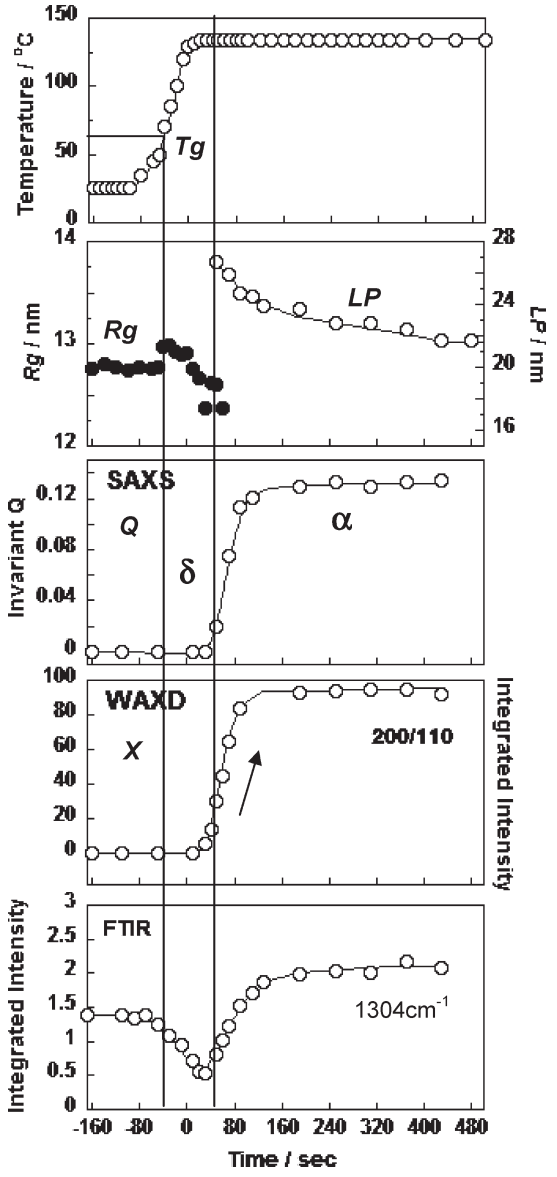

Figure 13. Time dependence of the radius of gyration (R_g), long period (LP), invariant (Q), degree of crystallinity (X) and 1304 cm^{-1} infrared band intensity estimated for PLLA mesophase measured in the isothermal crystallization process at T_c 130 °C, where the data were collected by performing the simultaneous measurements of transmission-FTIR, SAXS and WAXD data in BL40XU, SPring-8.

Figure 13 shows the time-dependences of the integrated intensity of the WAXD 200/110 reflection, the radius of gyration R_g and the long period LP estimated from the SAXS data at 130 °C. In this figure the integrated intensity of the infrared band at 1304 cm^{-1} is also plotted. As seen in Figure 12, the starting sample showed the band characteristic of the mesophase at 1304 cm^{-1}. As the time passaged, the bands intrinsic to the δ and α forms started to be detected. Since the separation of the overlapped bands was difficult, the band intensity in the 1325−1290 cm^{-1} region was estimated and plotted against the time in Figure 13. At the starting point the IR band at 1304 cm^{-1} was already relatively strong. As the temperature increased and crossed the T_g at about 40 s, this band intensity decreased once because of the decrease in the mesophase content, and then the

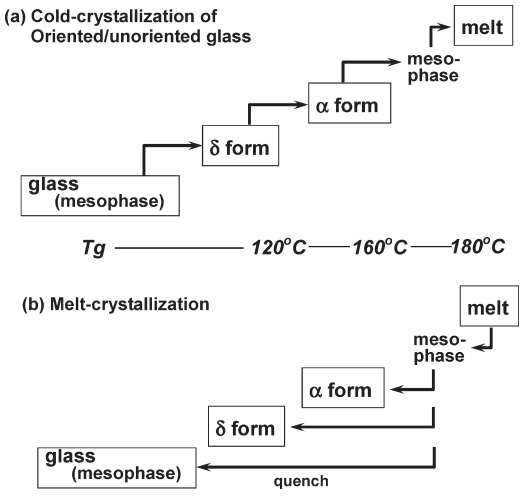

Figure 14. Schematic illustration of phase transitions of PLLA in the (a) cold- and (b) melt-crystallization processes.

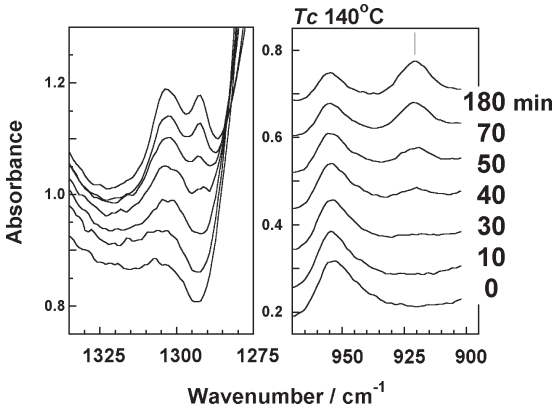

Figure 15. Time dependence of infrared spectra of PLLA measured in the isothermal crystallization process at T_c 140 °C from the melt.

band intensity increased again because the bands intrinsic to the crystalline phases increased instead. As seen in the SAXS data, the R_g of the mesophase nodule structure at room temperature was estimated to be 128 Å. Once the sample was heated up above T_g, it increased only slightly but discretely to 130 Å. As the temperature increased furthermore and at 50 s after the temperature reached T_c, the long period LP started to be detected, about 270 Å. In this figure the LP is almost equal to 2*Rg, suggesting the small domains of the mesophase approached each other and contacted together to form the stacked lamellar layers. With the passage of time the LP decreased gradually to 217 Å so that the lamellar stacking structure became tighter. The integrated intensity of the WAXD reflections is found to increase similarly with time. Figure 14a summarizes schematically the transition process from the mesophase to the melt through the formation of more regular δ and α forms on the way of heating. In this figure the mesophase is added just before the melt. This comes from the experimental data shown in Figure 7. It was reported that the X-ray layer-line reflections disappeared but the equatorial reflections were still observed in the similar temperature region immediately below the melting point,[44] consistent with the vibrational spectroscopic observation given in Figure 7.

dx.doi.org/10.1021/ma2017666 |*Macromolecules* 2011, 44, 9650–9660

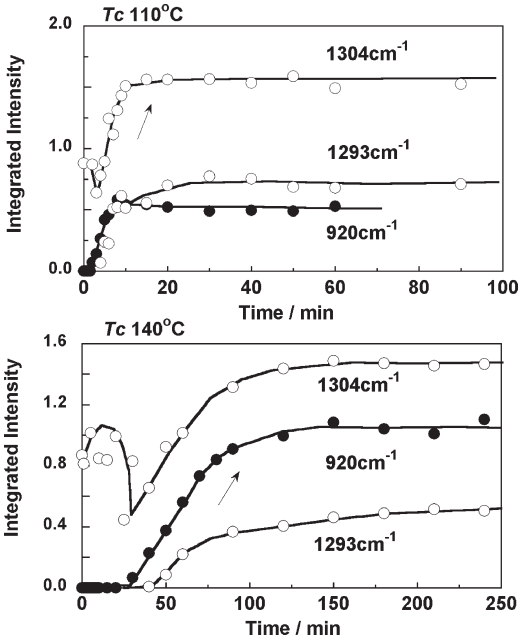

Figure 16. Time dependence of integrated intensity of the various infrared bands evaluated in the isothermal melt-crystallization processes at 110 and 140 °C.

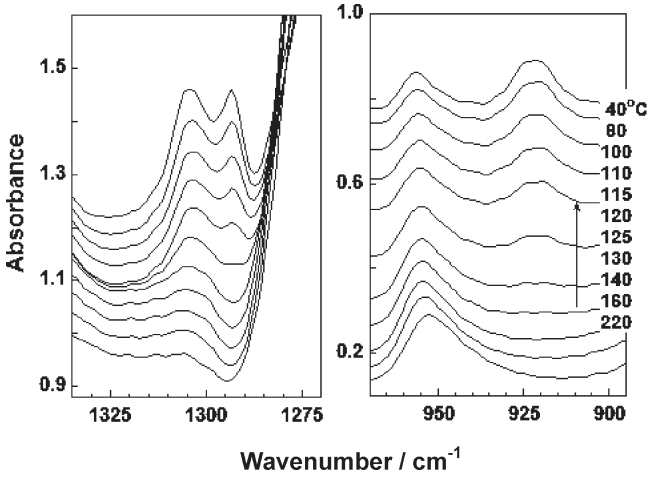

Figure 17. Temperature dependence of infrared spectra of PLLA sample measured in the nonisothermal cooling process from the melt.

Crystallization from the Melt. *Time Dependence.* The structural evolution in the isothermal crystallization from the melt was traced by measuring the rapid-scanning FTIR spectra as shown in Figure 15, where the case at T_c = 140 °C is reproduced. In the molten state the broad band at 1305 cm^{-1} was detected with the relatively low intensity. After the temperature jump to T_c = 140 °C, the 1304 cm^{-1} band increased in intensity at first. Then, at around 40 min after the jump, the bands at 920 and 1293 cm^{-1} increased in intensity in parallel as seen from the integrated intensity plot given in Figure 16. At T_c 110 °C, the behavior was almost similar to the case of 140 °C, but the band at 1297 cm^{-1} was relatively more intense than the band at 1304 cm^{-1}, different from the case at T_c 140 °C. It should be noticed here that the band at 1304 cm^{-1} increased the intensity immediately after the temperature jump. This broad but clear

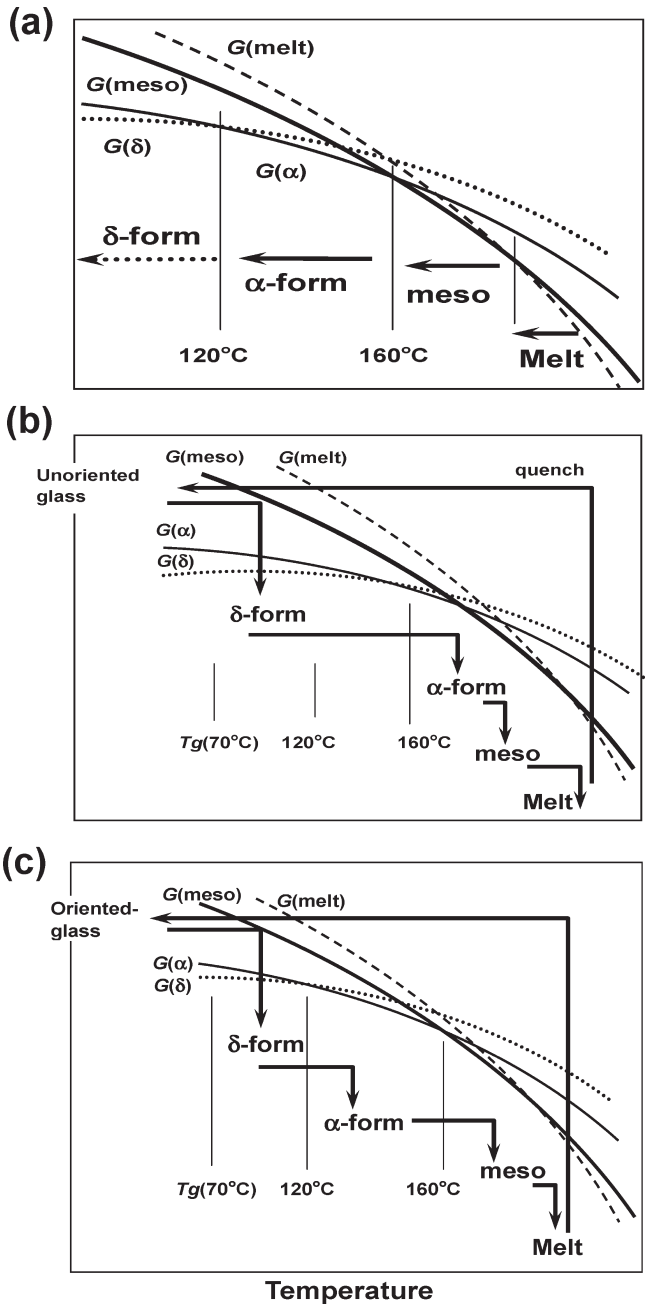

Figure 18. Gibbs free energy diagrams illustrated for (a) the melt-crystallization phenomenon of PLLA, (b) the cold-crystallization of unoriented PLLA sample, and (c) the cold-crystallization of oriented PLLA sample.

single band is essentially the same as that observed in the cold-crystallization experiment and can be assigned to the mesophase. Then we can deduce one important conclusion here about the isothermal crystallization from the melt: the random coils in the melt gather together to form the mesophase before the regularization into the α or δ form (see Figure 14b).

The integrated intensity of the 920 cm^{-1} band is plotted against the crystallization time in Figure 9b in comparison with the case of cold crystallization phenomena (part a). The T_c dependence is more remarkable for the melt-crystallization phenomenon than the case of cold-crystallization but the crystallization

dx.doi.org/10.1021/ma2017666 |*Macromolecules* 2011, 44, 9650–9660

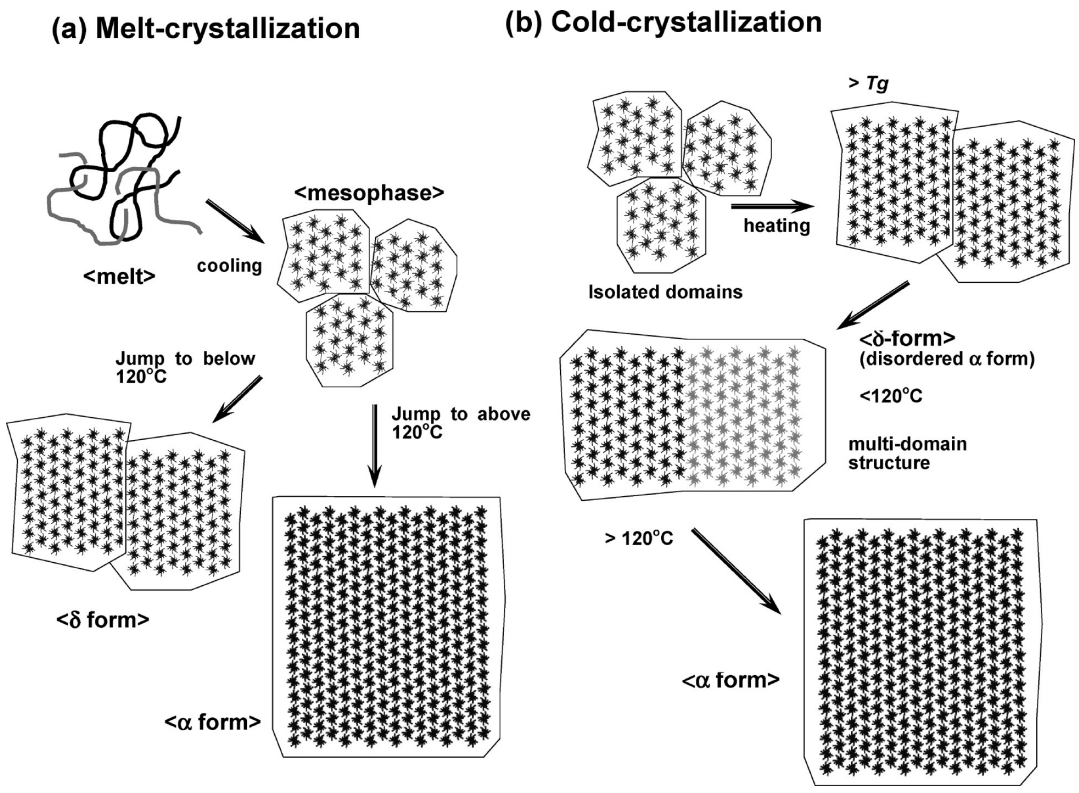

Figure 19. Schematic illustrations of structural evolution of PLLA in the (a) melt-crystallization and (b) cold-crystallization processes. The models are viewed along the chain axis. The small domains are gathered together to form the domains of larger size, where the structural regularization also occurs simultaneously about the chain conformation and chain packing mode in the crystal lattice. It is noticed here the domain size increases not only in the lateral directions but also along the chain axial direction.

rate itself is as a whole lower than the latter case. The crystallization constant k is plotted against T_c in Figure 10. In the temperature region of the formation of the δ form, the crystallization became maximal. This tendency is more remarkable in the cold crystallization compared with the melt-crystallization. In the latter case the formation of mesophase occurs in the melt followed by the regularization to the α form (or δ form), whereas the mesophase exists already in the cold crystallization case and the regularization and growth of the δ (and α) form occurs more easily.

Temperature Dependence. The temperature dependence of the FTIR spectra was measured to trace the structural change in the melt-crystallization process. Figure 17 shows the temperature dependence of IR spectra measured in the stepwise cooling process from the melt. The 1304 cm^{-1} band, which was weak in the molten state, became stronger during cooling and changed to the band of the mesophase. The band intensity became stronger furthermore, and then the band at 1293 cm^{-1} started to appear at around 120 °C. At the same time the crystalline-sensitive band at 920 cm^{-1} increased in intensity. In this case also the first generation of the mesomorphic phase can be confirmed in the cooling process from the melt, earlier than the regularization into the α form at around 120 °C.

Phase Transition Diagram. As mentioned in the preceding sections the crystallization behaviors of PLLA in the crystallization process from the molten state or amorphous glassy state were investigated by measuring the FTIR spectra as well as the WAXD and SAXS data as a function of time or temperature. All the data indicate clearly that the crystallization occurs *with the involvement of the mesomorphic phase.* Once the cold-crystallization starts from the melt-quenched glassy sample, then the generation of δ form occurs in the low temperature region near T_g followed by the transition to the regular α form in the higher temperature region. In the melt-crystallization process, on the other hand, the molten sample does not crystallize directly to the α or δ form from the melt, but the melt changes once to the mesophase and then it regularizes to the crystalline phase. These situations are already illustrated in Figure 14.

Figure 18 shows the Gibbs free energy diagrams showing the energetic relation between the melt, the mesophase and the crystalline α and δ forms. In the slow cooling process the melt changes to the mesophase at the crystallization temperature and then the mesophase transforms to the regular α form. Depending on the cooling rate from the melt, the α form does not appear but the disordered α or δ form appears instead. When the cooling rate is too high, the supercooling occurs and the mesophase is frozen at a low temperature below T_g (Figure 18b). This frozen mesophase immediately transforms to the δ form by thermally accelerating the chain motion above T_g. In this case, also the heating rate affects the generation of the crystalline form, the δ or α form.

As already mentioned, the oriented mesophase sample was prepared by stretching the melt-quenched sample at a temperature below T_g. As discussed in Figures 2 and 3, the X-ray diffraction data suggest that the mesophase consists of the parallel arrangement of the more-or-less disordered (10/3) helical chains with poor correlation in a small domain of several tens angstrom dimension. The heat treatment above T_g causes the regularization of the oriented mesophase to the oriented α or

δ form depending on the annealing temperature. In a separate paper we described the crystal structure of the δ form.[42] One of the most characteristic points is that this crystalline phase consists of the aggregation of relatively small domains and the relative height between the neighboring domains along the chain axis is statistically disordered, giving the continuous streak layer lines in the X-ray diffraction pattern. The inner structure of each domain is not very much deviated from that of the α form, although the structure is more or less disordered of course. The heat treatment at a higher temperature enhances the thermally activated translational motion of the chains and causes the *c*-axial shift of the neighboring domains so that the relative height becomes adjusted to give the α form of larger domain size. It is noticed here that such a regularization of domain aggregation is always accompanied by the further regularization in the chain conformation as well as the chain packing mode in the domain, resulting in the *phase* transition from the δ to α form. However, the thus-attained α form is not necessarily in a perfect single domain state but it still consists of the aggregation of domains of larger size. The relative height among these domains is still disordered, though slightly, to give the weak streaks along the layer lines in the X-ray diffraction pattern and also some deviation in the relative intensity between a series of 00*L* reflections from the values expected for the perfectly regular crystal structure, as described in the previous paper.[41] On the other hand, in the case of melt-crystallization phenomenon, the highly disordered mesophase appears at first, followed by the regularization to the crystalline phase. Figure 19 shows the schematic illustrations of these structural transitions between the melt, the mesophase, the δ form and the α form in the (a) melt-crystallilzation and (b) cold-crystallization phenomena of PLLA.

The transition from the δ (α′) form to the α form was reported to occur in the temperature region close to the melting point (around 160 °C) when the *unoriented* sample was used in the heating process from the room temperature.[44] On the other hand, as seen here also, the oriented δ (α′) form was observed to show the transition to the α form in such a low temperature as 120 °C. Why the transition from the δ to α form must occur in such largely different temperature regions between the oriented and unoriented samples? As described above, the phase transition between these phases is intimately related to the *c*-axial shift of the aggregated domains as well as the regularization of the conformation and packing mode of the helical chains, which are caused by the thermally accelerated translational chain motions along the chain axis. The forced parallel arrangement of the chains may cause such translational motion more easily due to some effect of residual tensile strain in the sample or due to the relatively smaller size of crystallites. The similar transition was reported for *isotactic* poly(butane-1) case, where the crystalline form II crystallized from the melt transforms to the form I at the very slow rate during the cooling process. But, once the oriented sample is used, the transition from form II to form I occurs for a quite short time.[52−55]

In this case also the parallel array of the chains is considered to enhance the cooperative translational motion of the chains more actively with lower energy barrier. The transition schemes given in Figure 18 take these situations also into account (parts b and c). The cold crystallization is not affected remarkably by such a difference in chain orientation.

CONCLUSIONS

In the present paper the structural regularizations of PLLA occurring in the crystallization processes from the melt and in the cold crystallization from the glassy state were described concretely on the basis of the temperature-dependent and time-dependent measurements of the FTIR spectra as well as the X-ray scattering data. In the cold crystallization from the glassy state, the mesomorphic state, which consists of the disordered aggregation of (10/3) helical chain segments in an appreciably small domain of several tens angstrom size, is regularized into the δ form. The aggregation of these small domains of the mesophase is not completed perfectly, but the resultant δ form domains are still statistically randomly disordered in the relative height along the chain axis although the degree of disorder is not very serious. Another important point to notice here is that the chain conformation of the δ form is appreciably irregular as understood from the lack of many even-numbered 00*L* reflections as reported before. The heat treatment in a temperature region higher than 120 °C induces the phase transition of the δ form into the α form of regular packing structure of regular helical chains. In this way, the cold crystallization from the mesophase is related to the enlargement of the domain size as well as the regularization of the chain conformation and chain packing mode. The mesophase is important in the melt-crystallization process also. The melt *does not transform directly* to the α or δ form, but it necessarily changes to the mesophase at first and then to the α or δ form with more regular crystal structure. If the cooling rate from the melt is too high, the disordered structure is frozen as the mesophase, which forms a kind of nodule structure with relatively ordered but tiny domains.

In the present paper, we did not discuss the relation between these structural regularization procedures and the morphology of the bulk sample. As reported in the literatures, the different morphology is obtained depending on the crystallization temperature: well-defined spherulites, coarse-grained spherulites, or axialites.[16,18,20,29−31] These morphologies might be related intimately to the formation process of the above-mentioned various types of the chain aggregation states.

ACKNOWLEDGMENT

The authors thank Professor Hideto Tsuji of Toyohashi University of Technology, Japan, for his kind supply of the sample. They also thank Drs. Hiroyuki Iwamoto, Noboru Ohta and Hiroyasu Masunaga of JASRI, SPring-8 for their kind supports in synchrotron experiments. They thank Drs. Tran Hai Ninh, Kummetha Raghunatha Reddy, Hiroko Yamamoto, and Taiyo Yoshioka of Toyota Technological Institute for their helpful discussion. This work was financially supported by the Strategic Project to Support the Formation of Research Bases at Private Universities of the Ministry of Education, Culture, Sports, Science and Technology, Japan (2010−2014).

REFERENCES

(1) Auras, R.; Harte, B.; Selke, S. *Macromol Biosci* **2004**, *4*, 835.
(2) Garlotta, D. *J .Polymer. Environ.* **2002**, *9*, 63.
(3) Mochisuki *Sen'I gakkaishi* **2010**, *66*, 70.
(4) Zhang, J.; Duan, Y.; Sato, H.; Tsuji, H.; Noda, I.; Yan, S.; Ozaki, Y. *Macromolecules* **2005**, *38*, 8012.
(5) Kawai, T.; Rahman, N.; Matsuba, G.; Nishida, K.; Kanaya, T.; Nakano, M.; Okamoto, H.; Kawada, J.; Usuki, A.; Honma, N.; Nakajima, K.; Matsuda, M. *Macromolecules* **2007**, *40*, 9463.
(6) Zhang, J.; Tashiro, K.; Domb, A. J.; Tsuji, H. *Macromol. Symp.* **2006**, *242*, 274.
(7) Cho, T. Y.; Strobl, G. *Polymer* **2006**, *47*, 1036.

(8) Mano, J. F. *J. Non-Cryst. Solids.* **2007**, *353*, 2567.
(9) Mano, J. F.; Wang, Y.; Viana, J. C.; Denchev, Z.; Oliveira, M. *J. Macromol. Mater. Eng.* **2004**, *289*, 910.
(10) Pan, P.; Kai, W.; Zhu, B.; Dong, T.; Inoue, Y. *Macromolecules* **2007**, *40*, 6898.
(11) Pan, P.; Liang, Z.; Zhu, B.; Dong, T.; Inoue, Y. *Macromolecules* **2008**, *41*, 8011.
(12) Zhou, Z. H.; Liu, X. P.; Liu, Q. Q.; Liu, L. H. *Int. J. Polym. Mater.* **2008**, *57*, 878.
(13) Wang, Y.; Funari, S. S.; Mano, J. F. *Macromol. Chem. Phys.* **2006**, *207*, 1262.
(14) Pan, P.; Zhu, B.; Kai, W.; Dong, T.; Inoue, Y. *Macromolecules* **2008**, *41*, 4296.
(15) Mahendrasingam, A.; Blundell, D. J.; Parton, M.; Wright, A. K.; Rasburn, J.; Narayanan, T.; Fuller, W. *Polymer* **2005**, *46*, 6009.
(16) Vasanthakumari, R.; Pennings, A. J. *Polymer* **1983**, *24*, 175.
(17) Iannace, S.; Nicolais, L. *J. Appl. Polym. Sci.* **1997**, *64*, 911.
(18) Di Lorenzo, M. L. *Eur. Polym. J.* **2005**, *41*, 569.
(19) Di Lorenzo, M. L. J. *Appl Polym Sci* **2006**, *100*, 3145.
(20) Zhou, Z.-H.; Ruan, J.-M.; Zhou, Z.-C.; Zou, J.-P. *Polym.-Plast. Technol.* **2007**, *46*, 863.
(21) Ling, X.; Spruiell, J. E. *J. Polym. Sci., Polym. Phys.* **2006**, *44*, 3200.
(22) Shieh, Y. T.; Liu, G.-L. *J. Polym. Sci., Polym. Phys.* **2007**, *45*, 466.
(23) He, Y.; Fan, Z.; Hu, Y.; Wu, T.; Wei, J.; Li, S. *Eur. Polym. J.* **2007**, *43*, 4431.
(24) Yasuniwa, M.; Iura, K.; Dan, Y. *Polymer* **2007**, *48*, 5398.
(25) Sanchez, M. S.; Mathot, V. B. F.; Poel, G. V.; Ribelles, J. L. G. *Macromolecules* **2007**, *40*, 7989.
(26) Wu, L.; Hou, H. *J. Appl. Polym. Sci.* **2010**, *115*, 702.
(27) Ohtani, Y.; Okumura, K.; Kawaguchi, A. *J. Macromol. Sci., Phys. B* **2003**, *42*, 875.
(28) Di Lorenzo, M. L.; Cocca, M.; Malinconico, M. *Thermochim. Acta* **2011**, *522*, 110.
(29) Wang, Y.; Gómez Ribelles, J. L.; Salmerón Sánchez, M.; Mano, J. F. *Macromolecules* **2005**, *38*, 4712.
(30) Miyata, T.; Masuko, T. *Polymer* **1998**, *39*, 5515.
(31) Yuryev, Y.; Wood-Adams, P.; Hevzey, M.-C.; Dubois, C.; Brisson, J. *Polymer* **2008**, *49*, 2306.
(32) Stoclet, G.; Seguela, R.; Lefebvre, J. M.; Elkoun, S.; Vanmansart, C. *Macromolecules* **2010**, *43*, 1488.
(33) Stoclet, G.; Seguela, R.; Lefebvre, J.-M.; Rochas, C. *Macromolecules* **2010**, *43*, 7228.
(34) Zhang, J.; Duan, Y.; Domb, A. J.; Ozaki, Y. *Macromoleculse* **2010**, *43*, 4240.
(35) Aou, K.; Kang, S.; Hsu, S. L. *Macromolecules* **2005**, *38*, 7730.
(36) Allegra, G., Ed. *Advances in Polymer Science*; Springer: Berlin, 2005; Vol. 180.
(37) Yang, X.; Kang, S.; Yang, Y.; Aou, K.; Hsu, S. L. *Polymer* **2004**, *45*, 4241.
(38) Zhang, J.; Tsuji, H.; Noda, I.; Ozaki, Y. *J. Phys. Chem. B* **2004**, *108*, 11514.
(39) Zhang, J.; Tsuji, H.; Noda, I.; Ozaki, Y. *Macromolecules* **2004**, *37*, 6433.
(40) Pan, P.; Zhu, B.; Kai, W.; Dong, T.; Inoue, Y. *J. Appl. Polym. Sci.* **2007**, *107*, 54.
(41) Wasanasuk, K.; Tashiro, K.; Hanesaka, M.; Ohhara, M.; Kurihara, K.; Kuroki, R.; Tamada, T.; Ozeki, T.; Kanamoto, T. *Macromolecules* **2011**, *44*, 6441.
(42) Wasanasuk, K.; Tashiro, K. *Polymer*, in press.
(43) Yasuniwa, M.; Sakamo, K.; Ono, Y.; Kawahara, W. *Polymer* **2008**, *49*, 1943.
(44) Zhang, J.; Tashiro, K.; Tsuji, H.; Domb, A. J. *Macromolecules* **2008**, *41*, 1352.
(45) Zhang, J.; Li, C.; Duan, Y.; Domb, A. J.; Ozaki, Y. *Vib. Spectrosc.* **2010**, *53*, 307.
(46) Sasaki, S.; Tashiro, K.; Kobayashi, M.; Izumi, Y.; Kobayashi, K. *Polymer* **1999**, *40*, 7125.
(47) Strobl, G. *Prog. Polym. Sci.* **2006**, *31*, 398.
(48) Alexander, L. L. *X-ray Diffraction Methods in Polymer Science*; John Wiley & Sons: New York, 1969.
(49) Tashiro, K.; Yoshioka, T.; Yamamoto, H.; Ninh, T. H.; Shimada, S.; Nakatani, T.; Iwamoto, H.; Ohta, N.; Masunaga, H. *Polym. Prepr. Jpn.* **2011**, *60*, 2M05.
(50) Feigin, L. A.; Svergun, D. I. *Structure Analysis by Small-Angle X-ray and Neutron Scattering*; Plenum Press: New York, 1987.
(51) Reddy, K. R.; Tashiro, K; Sakurai, T; Yamaguchi, N; Sasaki, S; Masunaga, H; Takata, M. *Macromolecules* **2009**, *42*, 4191.
(52) Gohil, R. M.; Miles, M. J.; Petermann, J. *J. Macromol. Sci., Phys. B* **1982**, *21*, 189.
(53) Kopp, S.; Wittman, J. C.; Lotz, B. *J. Mater. Sci.* **1994**, *29*, 6159.
(54) Marigo, A.; Marega, C.; Cecchin, G.; Collina, G.; Ferrara, G. *Eur. Polym. J.* **2000**, *36*, 131.
(55) Maruyama, M.; Sakamoto, Y.; Nazaki, K.; Yamamoto, T.; Kajioka, H.; Toda, A.; Yamada, K. *Polymer* **2010**, *51*, 5532.